Structure-Property Relationships of an Electron Beam Cured Model Urethane Prepolymer

EUGENE JOSEPH and GARTH WILKES, *Department of Chemical Engineering, Virginia Polytechnic Institute and State University, Blacksburg, Virginia 24061*, and KISOON PARK, *Union Carbide Corporation, P.O. Box 8361, South Charleston, West Virginia 25303*

Synopsis

A semicrystalline urethane prepolymer derived from polycaprolactone was crosslinked below and above the melt to different levels using electron beam radiation. Studies at room temperature on the systems crosslinked under ambient conditions, which is below the melting temperature, show that changes in mechanical properties which occur as the electron beam dose is increased are due principally to the increase in crosslink density and to the changes in the crosslinking mechanism. Specifically, crosslinking takes place mainly at the acrylate double bonds or may also occur along the polymer backbone. All systems, however, are semicrystalline and possess a spherulitic texture. Mechanical and rheo-optical testing above the melt on these same systems indicate that at extensions up to 125% classical rubber elasticity theory and photoelasticity theory is obeyed. Isothermal crystallization kinetics measurements show that the rate of crystallization decreases as the electron beam dose is raised. When the systems are crosslinked above the melt again a spherulitic texture results. Mechanical testing above the melting temperature on the prepolymer crosslinked up to 4 Mrad shows that at elongations up to 125% classical rubber elasticity theory is obeyed. At room temperature these latter crosslinked systems exhibited a lower modulus compared to the materials crosslinked below the melt. Polarizing optical microscopy carried out above the melting temperature strongly suggested that no order was present in these systems during crosslinking in contrast to those crosslinked below the melting temperaure.

INTRODUCTION

Since the time that polymers have been applied as coating materials, there has been interest in two particular aspects of their behavior with respect to their exposure to various forms of high energy radiation. While early interest focused on how radiation altered the end-use properties, more recently much effort has been directed at utilizing visible, UV, and electron beam radiation as a means of polymerization (curing by crosslinking) of coatings and films, etc. One of the classes of materials that are utilized as coatings are polyurethanes, and they are usually linear polymers applied from a 20–30% solution and are cured thermally.[1] However, with the rapid increase in solvent and energy costs, the trend has been to increase the percent solids, and withing the last 10–15 years, several 100% solids polyurethane systems have been designed for coating applications. 100% solids coating may be defined as 100% reactive compositions that are essentially free of volatile solvents at the time of cure and contain diluent molecules that react during the curing process to become part of the final coating. By using 100% solids systems in conjunction with electron beam radiation for crosslinking, great savings in energy can be made.[2,3] More specifically, a given wavelength or a selection of wavelengths of electron beams speed up the dissociation of the free

Journal of Applied Polymer Science, Vol. 26, 3355–3376 (1981)
 CCC 0021-8995/81/103355-22$02.20

radical source, and it is due to this initiation step of the curing of 100% solids systems that the great energy advantages of the electron beam technique come into play. Details of the electron beam curing technology and chemical reaction mechanism are mentioned elsewhere.[4,5] Rather, this paper deals with the mechanical and morphological studies of a semicrystalline urethane prepolymer, which was crosslinked below and above the crystalline melting point at various electron beam doses. The properties of these networks were studied both below and above the melting temperature. It might be pointed out that, to our knowledge, this study is one of the few structure-property investigations that have been carried out on this class of coating materials.

MATERIALS

The model prepolymer was synthesized in three steps. In the first step, two equivalents of poly(caprolactone diol) ($\overline{M}_w$ = 3100) were reacted with 1.1 equivalents of isophoronediisocyanate (IPDI) to form a chain extended diol. An isocyanate-capped intermediate was obtained by the reaction of 1 equivalent of the chain-extended diol and 2.1 equivalents of IPDI. In the final step, the reaction between the isocyanate-capped intermediate and hydroxy ethylacrylate produced the model prepolymer.[6,7] The chemical structures of the diol, isocyanate-capped intermediate, and model prepolymer are shown in Figure 1.

Crosslinking of the prepolymer film was carried out (external conditions) at room temperature and at 60°C, which respectively correspond to below and above the crystalline melting temperature of the prepolymer. The melting temperature is on the order of 50°C. The chain-extended diol and the isocyanate-capped intermediate irradiated at different electron beam doses were also obtained. Single pass electron beam doses ranging from 0.5 Mrad to 16 Mrad were utilized for crosslinking where 1 rad is defined as 100 ergs of energy absorbed by 1 g of material.[7] Network systems were also obtained by crosslinking the prepolymer mixed with four different levels of 1,6-hexanedioldiacrylate (HDDA), at an electron beam dose of 4 Mrad. HDDA is a tetrafunctional crosslinker.

EXPERIMENTAL

Mechanical testing at room temperature (i.e., below the melting temperature) was performed using an Instron Model 1122. A Ladd Tensile Holder in conjunction with a thermal chamber was used for mechanical testing above the melting temperature. Birefringence measurements and small angle light scattering patterns were obtained using procedures described elsewhere.[8] Polarizing microscopy studies were made using a Zeiss Standard RP Polarizing Microscope in conjunction with a Mettler FP2 Hot Stage. Crystallization kinetics studies were performed using the same optical microscope and hot stage, along with a photodiode eyepiece in order to monitor the magnitude of the depolarization that occurred due to crystallization. A schematic of this apparatus is shown in Figure 2. A ISI Super III- A Scanning Electron Microscope was used for morphological investigations, while a Dupont 990 Thermoanalyzer was utilized for DSC measurements.

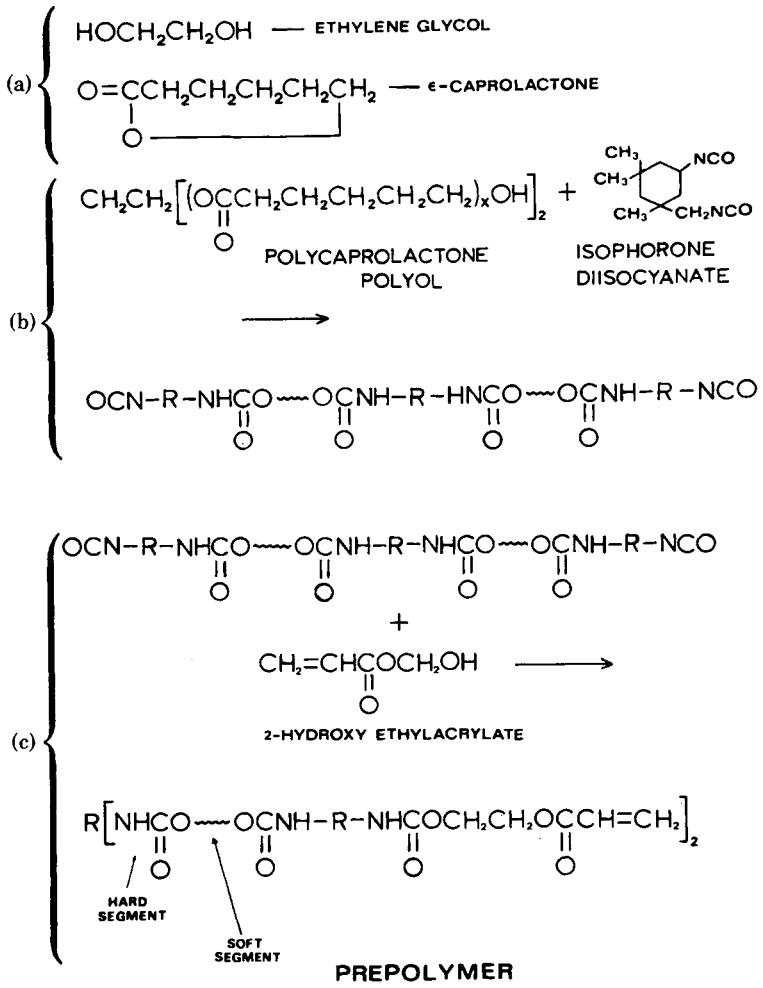

Fig. 1. (a) Reactants used to produce polycaprolactonediol; (b) chemical reaction involved in producing the isocyanate capped intermediate; and (c) chemical reaction involved in the synthesis of the final prepolymer. R is the cycloaliphatic portion of isophorone diisocyanate. ~~ represents the polycaprolactonediol segment.

RESULTS AND DISCUSSION

Properties of Prepolymer Crosslinked at Ambient Conditions

Gel fraction measurements on the prepolymer showed that the gel fraction content increases rapidly to a value of about 0.99 at 1 Mrad and as irradiation dose increases to 12 Mrad there is a slight decrease in gel fraction (see Fig. 3a). This decrease is likely due to chain scission occurring at these high electron beam doses. In order to obtain a better understanding of the crosslinking process, only the chain-extended diol and the isocyanate-capped intermediate were crosslinked at various electron beam doses at room temperature and the gel fractions were measured. As shown in Figure 3b, the gel fraction content increases with irradiation dose, and at irradiation doses greater than 4 Mrad the increase is much more significant. This increase in gel fraction must be attributed to crosslinking along the polymer chain backbone since the units making up the chain do not

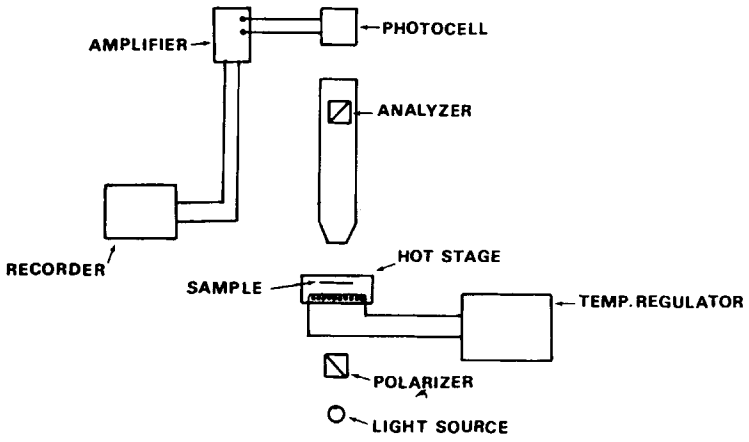

Fig. 2. Apparatus used to measure fluctuations in depolarized light intensities during crystallization studies.

contain any acrylate double bonds. It is speculated that at electron beam doses up to 4 Mrad crosslinking occurs mainly at the acrylate double bonds which are excluded from the polycaprolactone crystal lattice. However, at higher irradiation doses enough energy exists for some additional crosslinking to take place inside the crystal lattice, when crosslinking occurs below the melting temperature.*

Differential scanning calorimetry (DSC) was used in this study to obtain the melting temperature (T_m) and the heat of fusion (ΔH_f). The melting temperature and the heat of fusion ranged from 48°C to 52°C and 12.4 cal/g to 10.0 cal/g, respectively, with the lower T_m and ΔH_f corresponding to materials exposed to higher dosage. The parameters of T_m and ΔH_f were obtained as a function of irradiation dose and are given in Table I. At low electron beam doses (0.5 Mrad and 4 Mrad) there is very little change but, at higher electron beam doses (8 Mrad and 12 Mrad), T_m and ΔH_f have lower but not widely varying values. This decrease in T_m and ΔH_f is likely due to the increase in the number of crosslinks with electron beam dose, which act as defects or imperfections in the crystal structure. Another reason for this decrease in T_m and ΔH_f may be due to the induced melting caused by the crosslinking process at higher irradiation doses. This will be discussed further in the section regarding morphological studies.

Mechanical and Rheo-optical Studies above the Melt (60°C)

Mechanical testing was performed on the ambient crosslinked systems at 60°C and the stress–strain plots are shown in Figure 4. The modulus increases from 4×10^5 Pa to 9×10^5 Pa, as the electron beam dose is increased up to 10 Mrad. These values clearly indicate rubbery behavior. This increase in modulus can

* The reviewer offered an alternate possibility, i.e., the beam-heating at high doses reduced the prepolymer viscosity and hence increased the number of radical terminations. The reviewer's remark is well taken by the authors. Experiments are needed, however, to proof either proposal.

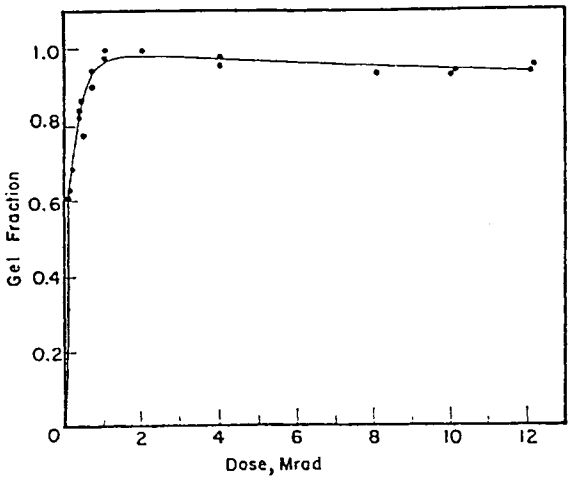

(a)

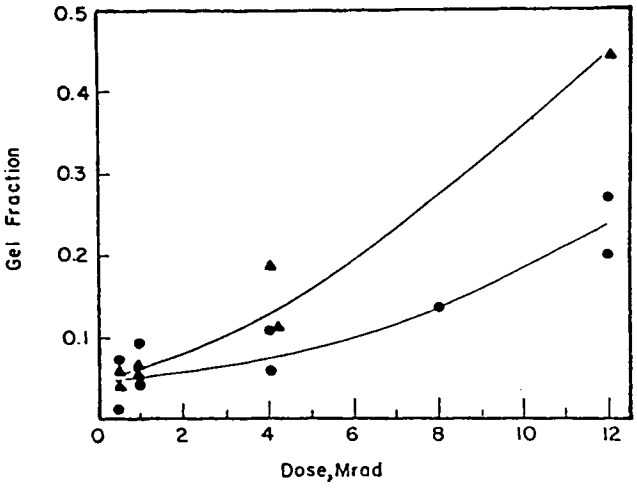

(b)

Fig. 3. Plot of gel fraction vs. electron beam dose for: (a) final prepolymer, (b) polycaprolactone and isocyanate-capped intermediate. (●) PCL–polyol, (▲) NCO–capped prepolymer.

be directly attributed to further crosslinking as radiation dose is increased. However, as radiation dose is increased up to 16 Mrad, there is a decrease in modulus. It is apparent that at these high electron beam doses chain scission may occur and serve somewhat to reduce the modulus.

TABLE I
Results of Differential Scanning Calorimetry Experiments

Irradiated prepolymer	Melting point (°C)	Heat of fusion (cal/g)
At 0.5 Mrad	53.1	12.4
At 4 Mrad	53.3	12.4
At 8 Mrad	49.2	10.5
At 12 Mrad	49.2	10.0

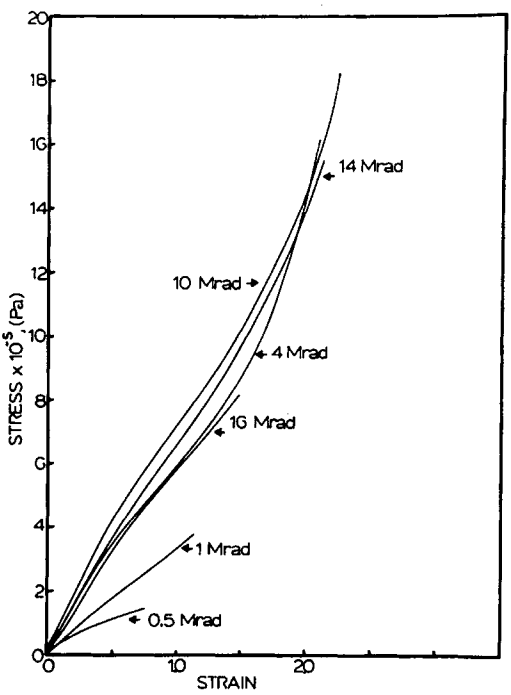

Fig. 4. Stress vs. strain curves above the melting temperature of the 0.5 Mrad, 1 Mrad, 4 Mrad, 10 Mrad, 14 Mrad, and 16 Mrad materials which were crosslinked at room temperature.

Since the experiment was performed in the melt state, the effect of initial crystallinity does not exist. The system might be regarded as a rather typical network system. Because of this, and in view of the observed moduli, the stress–strain data were replotted in the classical rubber elasticity equation,[9]

$$\sigma = N_v kT(\lambda - 1/\lambda^2) \tag{1}$$

where σ is the engineering stress, N_v is the number of network chains per unit volume, k is Boltzmann's constant, T is absolute temperature, and λ is the extension ratio. The plot of stress vs. $(\lambda - 1/\lambda^2)$ is shown in Figure 5, and the straight lines indicate that these systems clearly follow classical rubber elasticity theory well up to about 125% elongation. At higher elongations, classical rubber elasticity theory does not hold. The slopes obtained from the straight lines provide the calculation of the crosslink density, i.e.,

$$N_v = \rho RT/M_c \tag{2}$$

and hence, the molecular weight between crosslinks ($\overline{M}_c$). The gas constant is given by R while ρ represents the density. These results are given in Table II and are in agreement with the behavior of the moduli mentioned earlier, i.e., lower $\overline{M}_c$ for higher dosage.

Extension–retraction experiments above the melt in the range where classical rubber elasticity theory holds show mechanical hysteresis behavior that is the same order of magnitude to more classical elastomeric materials.[9] For example, at an 85% elongation, crosslinked polybutadiene at 25°C, which is a good elastomeric material, was determined to have a 9% hysteresis while the 8-Mrad

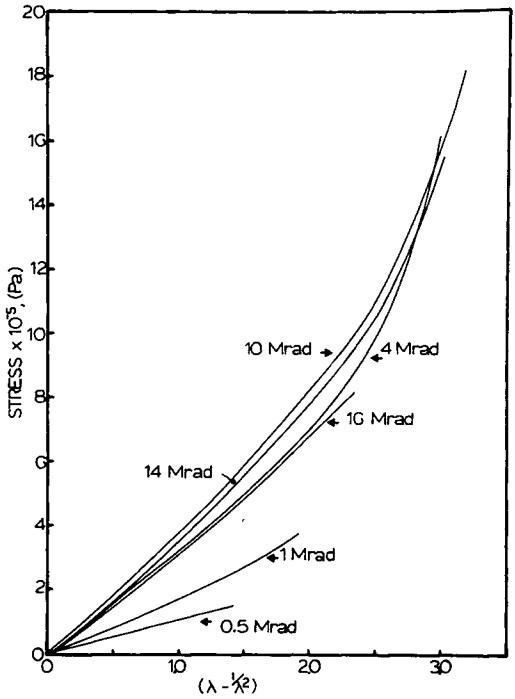

Fig. 5. Stress vs. $(\lambda - 1/\lambda^2)$ plot, from stress–strain data obtained above the melting temperature of the 0.5 Mrad, 1 Mrad, 4 Mrad, 10 Mrad, 14 Mrad, and 16 Mrad materials which were crosslinked at room temperature.

sample at 60°C also for the same loading scheme also has a 9% hysteresis. In view of the speculated prepolymer model (see below), these results are found to be a bit surprising. Specifically, the over simplified molecular model of the prepolymer is shown in Figure 6, where the polycaprolactonediol segments lie principally within crystallites while the urethane segment and the acrylate double

TABLE II
Results of Mechanical Testing above Melting Temperature

Material	Modulus (Pa)	Molecular weight between crosslinks (M_c)
Prepolymer crosslinked at room temperature:		
(a) 0.5 Mrad	2.97×10^5	2.315×10^4
(b) 1 Mrad	3.72×10^5	1.473×10^4
(c) 4 Mrad	7.43×10^5	0.772×10^4
(d) 10 Mrad	8.32×10^5	0.655×10^4
(e) 14 Mrad	7.17×10^5	0.705×10^4
(f) 16 Mrad	6.21×10^5	0.805×10^4
Prepolymer crosslinked in the melt state:		
(g) 0.5 Mrad/Liq*	4.52×10^5	1.350×10^4
(h) 1 Mrad/Liq	5.94×10^5	0.836×10^4
(i) 4 Mrad/Liq	8.32×10^5	0.579×10^4

* Liq indicates that the samples were crosslinked in liquid form.

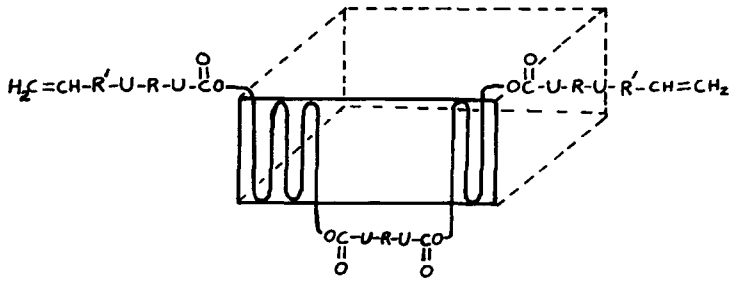

Fig. 6. Speculated molecular model of prepolymer. The polycaprolactone segments lie within the crystallite while the urethane segment and the acrylate double bonds are excluded. U represents the urethane linkage, R the cycloaliphatic portion of isophorone diisocyanate, and R′ represents $(OCCH_2CH_2OC)$.

bonds are excluded. Since at low irradiation doses crosslinking takes place mainly at location of the double bonds and hence outside the crystal lattice, it is expected that a network with a nonrandom crosslink density would result. This would suggest that even at low elongations classical rubber elasticity theory may not be satisfied and that a larger amount of hysteresis may be present. However, as is clear from the earlier data in Figure 5, agreement with classical theory is quite satisfying at least to somewhat over 100% elongation.

Turning to a different mechanical parameter, the results of stress–relaxation measurements above the melt and at 50% elongation are shown in Figure 7. The prepolymer irradiated at low and high electron beam doses shows almost no stress decay over a period of approximately 3 h. These results seem to be reasonable in terms of the speculated model and the type of chain chemistry. Specifically, at low electron beam doses, relaxation due to entanglements of dangling long chain molecules does not occur. This is because crosslinking of chain ends occurs, and, hence, dangling chain ends most probably are not present in significant quantity in the network. At higher doses, in addition to crosslinking of the chain ends, crosslinking along the polymer backbone also takes place again preventing the relaxation of the molecules. However, high dosage also complicates the above simplistic picture due to the inducement of some chain scission which, of course, can provide dangling ends.

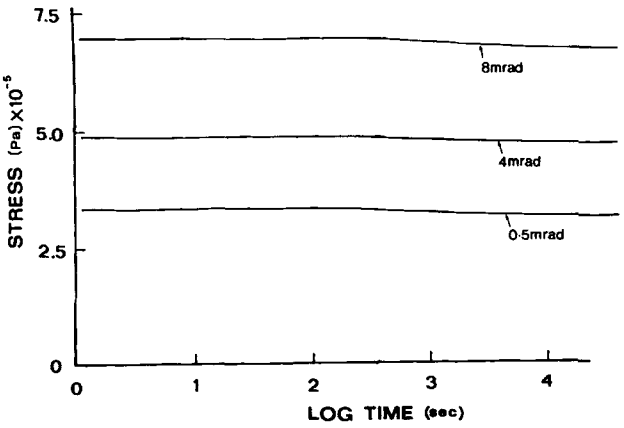

Fig. 7. Plot of stress time for the 0.5 Mrad, 4 Mrad, and 8 Mrad materials above the melting temperature in a stress relaxation experiment for $\lambda = 1.5$.

Mechanical testing was also performed above the melt on samples containing the tetrafunctional crosslinker and irradiated at 4 Mrad. The stress–strain curves are shown in Figure 8, and, as expected, the modulus and tensile strength are raised as the amount of HDDA is increased. The increase in modulus is due to the higher degree of crosslinking. These latter stress–strain data, when plotted in the classical rubber elasticity equation, provide Figure 9. There it is observed that these materials do not obey classical rubber elasticity theory in that they are nonlinear even at low elongations. This is presently accounted for as due to the increased crosslinking which leads to a more non-gaussian network. That is, through additional crosslinking along the backbone in excess of the end vinyl groups, the decrease in molecular weight between crosslinks will clearly place many of the network chains into a non-gaussian region. We believe it is these short network chains that principally cause this deviation. Extension–retraction experiments performed on these networks show that as the level of crosslinker is raised there is also an increase in mechanical hysteresis. This behavior may well also be coupled to the limits of deformation caused by the non-gaussian network chains suggested above.

For further verification of classical rubber elasticity behavior, or the degree of deviation from, use of the rheo-optical method of birefringence was applied to these same materials. Figure 10 shows the birefringence measured above the melting temperature as a function of time following stretching to a 50% elongation for systems without HDDA. It is noted that the birefringence stays constant over a considerable period of time, indicating that there is very little change in orientation. The stress optical coefficient (SOC), defined as the ratio of birefringence to actual stress, was utilized to verify if the materials followed classical photoelasticity theory. At an elongation of 50%, the SOC remains constant over a period of time, further supporting the earlier statements that these systems

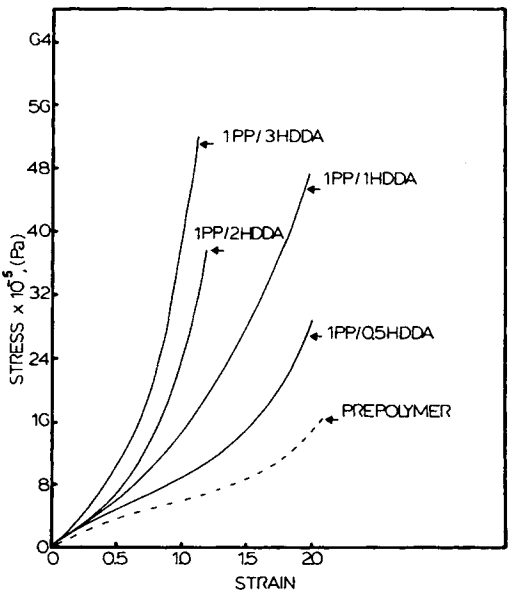

Fig. 8. Stress vs. strain curves above the melting temperature of the prepolymer containing 0 mol HDDA, 0.5 mol HDDA, 1 mol HDDA, 2 mol HDDA and 3 mol HDDA, and irradiated at 4 Mrad.

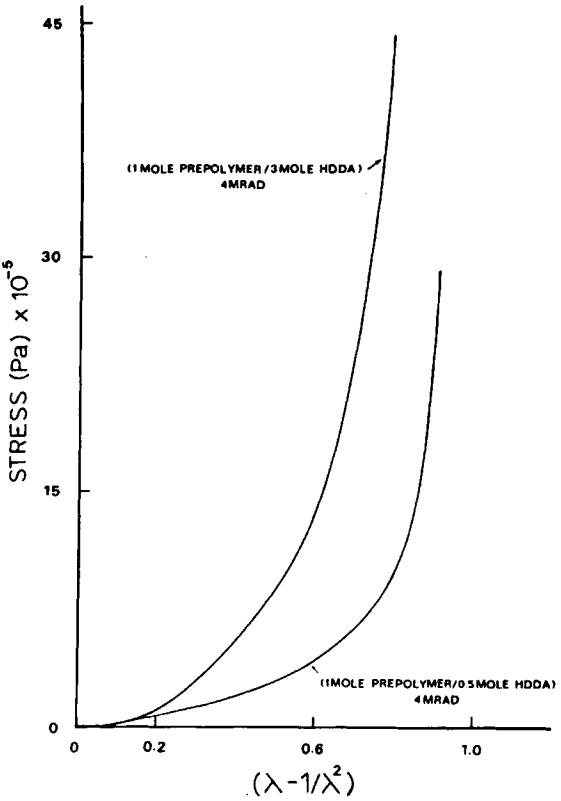

Fig. 9. Stress vs. $(\lambda - 1/\lambda^2)$ plot above the melting temperature of the prepolymer containing 0.5 mol HDDA and 3 mol HDDA, and irradiated at 4 Mrad.

satisfy classical rubber elasticity theory. These data also lend further support to the earlier proposed model that the initial radiation dosage will lead to crosslinks formed by coupling through the ends of the prepolymer vinyl groups. That is, this will provide a network, in principle, with no or few dangling chains. Hence, upon deformation, one would expect little decay in orientation if such dangling chains are in minimal concentrations.

Mechanical Studies Carried Out below the Melt

Figure 11 shows the stress–strain plot of the ambient crosslinked systems when the experiment was performed at room temperature. The differences in yield point peak behavior can be qualitatively explained in terms of the speculated morphological structure of the prepolymer mentioned earlier in this paper. Focusing initially on the stress–strain curves of the 0.5-Mrad, 2-Mrad, and 4-Mrad samples, it is seen that, as irradiation dose is increased up to 2 Mrad, the yield stress increases. However, the 4-Mrad material has a lower yield stress than that of the 2-Mrad material. The increase in yield stress is believed to be due to the increase in crosslinking mainly occurring at the double bonds. The decrease in yield stress at 4 Mrad is attributed to the effects of crosslinking inside the crystal lattice which partially disrupts the ordered crystal structure and hence affects deformation behavior. It is also found that at higher irradiation doses

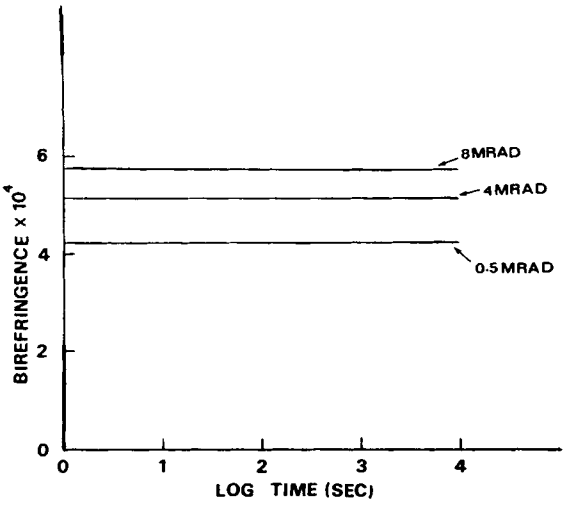

Fig. 10. Plot of birefringence vs. time for 0.5 Mard, 2 Mrad, and 8 Mrad samples above the melting temperature for $\lambda = 1.5$.

(e.g., 10 Mrad), there is a more significant change in the shape of the stress–strain curve. Specifically, a yield stress that is approximately 40% lower than that of the 4-Mrad material is observed while the sharp yield point peak is in fact no longer present. Initial energy balance calculations indicated that at electron beam doses greater than 8 Mrad enough energy was placed into the system to likely induce melting. That is, when the energy required to raise the material to its melting temperature is added to the heat of fusion and then compared to the energy of the electron beam at various doses, it was found that, at irradiation doses greater than 8 Mrad, enough energy was present to melt the crystals. (In this first-order energy balance calculation, no account was made for the energy changes caused by the opening of the double bonds.) It is speculated that the major change in the shape of the stress–strain curve is due to the induced melting at high electron beam doses (e.g., 10 Mrad), which may also cause a change in the overall crystalline morphology. This speculation was supported by obtaining

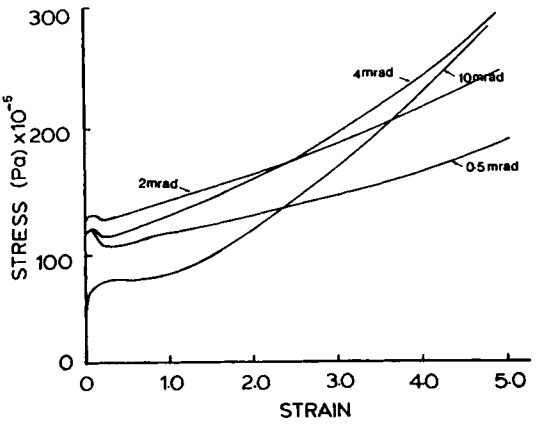

Fig. 11. Stress vs. strain curves at room temperature (i.e., below melting temperature) of the prepolymer irradiated at 0.5 Mrad, 2 Mrad, 4 Mrad, and 10 Mrad.

the stress–strain curve of a low dosage (0.5-Mrad) sample that was first melted and recrystallized prior to the stress–strain experiment. This material had similar stress–strain behavior to that of the 10-Mrad material and is shown in Figure 12. Hence, it is possible to conclude that the induced melting does cause a change in the mechanical properties.

As expected, stress–strain experiments on the materials containing HDDA showed that the modulus increases as the level of HDDA is raised. This is due to an increase in the degree of crosslinking.

Morphological Studies on Ambient Crosslinked Materials

Mechanical testing performed at room temperature suggested that changes in the mechanical properties are likely coupled with changes in morphology. Hence, morphological studies using microscopy and SALS were performed on samples having different electron beam dosages.

The H_v SALS pattern of the prepolymer cast from toluene is shown in Figure 13. The four-leaf clover pattern characteristic of an anisotropic spherulitic structure is observed and the bands surrounding the cloverleaf pattern arise from a banded spherulitic texture, i.e., periodic twisting or oscillation the lamella.[10] The irradiated materials also showed distinct spherulitic structure, but the SALS patterns could not be easily recorded photographically apparently due to considerable multiple scattering, i.e., higher turbidity caused by the thicker films. However, the basic H_v pattern was still observed in the high scattering background. Due to the limitations of the SALS in these studies, use of SEM procedures were also employed.

Scanning electron micrographs of the prepolymer and the prepolymer irradiated at 0.5 Mrad, 10 Mrad, and 16 Mrad are shown in Figure 14. All four micrographs clearly show spherulitic structure, but the surface texture was distinctly more fibrous for the 10-Mrad compared to the prepolymer and 0.5-Mrad materials. This change in surface texture was speculated to possibly be due to melting during the crosslinking process at higher electron beam doses. That is, at electron beam doses greater than 8 Mrad there is enough energy to melt the crystals

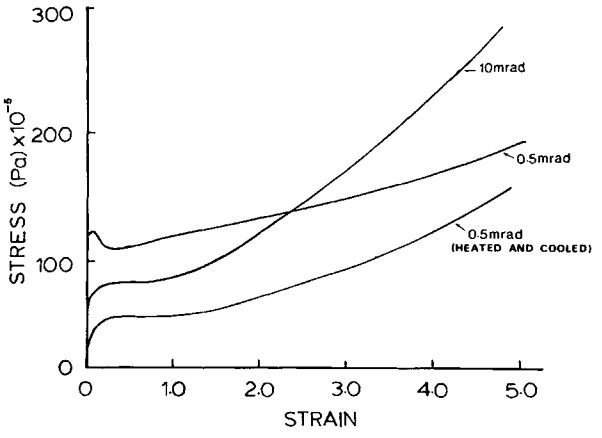

Fig. 12. Stress vs. strain curve at room temperature of the melted and recrystallized 0.5-Mrad material compared with the initial 0.5-Mrad and 10-Mrad materials.

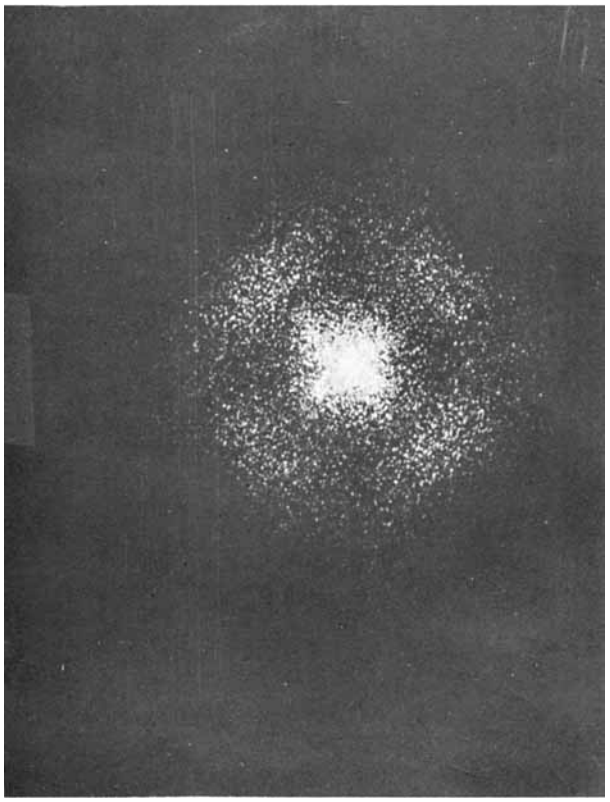

Fig. 13. H_v small angle light scattering pattern of the prepolymer cast from toluene.

and on recrystallization a different texture is obtained. This was supported by the SEM micrograph of a 0.5-Mrad sample that was melted and then recrystallized at room temperature. Figure 15 shows that this material does not have the same smooth texture of the original 0.5-Mrad film and in fact is quite similar to the 10-Mrad material. This strongly implies that the change in morphological texture at irradiation doses greater than 8 Mrad may be due to the melting of the polymer due to irradiation followed by recrystallization.

One of the applications of these or related systems under study would be as a binder for nonwovens or other semideformable systems. Hence, the deformation behavior followed by its recovery is of importance. As a result of this and because of the distinct superstructure texture, morphological studies of the deformed systems were briefly conducted by SEM methods. Figure 16 shows the electron micrographs of the 0.5-Mrad and 12-Mrad materials that had been deformed to 270% and 200%, respectively, at room temperature. Both show similar structure in that the spherulites are deformed into ellipsoids with their long axes along the stretch direction. When these deformed films were annealed at 40°C (T_m is the order of 50°C) for 10 min, the higher dosage sample shows a 65% recovery while the lower dosage material shows a 26% recovery. The higher strain recovery shown by the 12-Mrad sample is certainly due to the higher crosslinking which promotes higher entropic retraction forces and at the same time limits the loss of strain by molecular flow.

Polarizing optical microscopy was performed above the melt in order to obtain

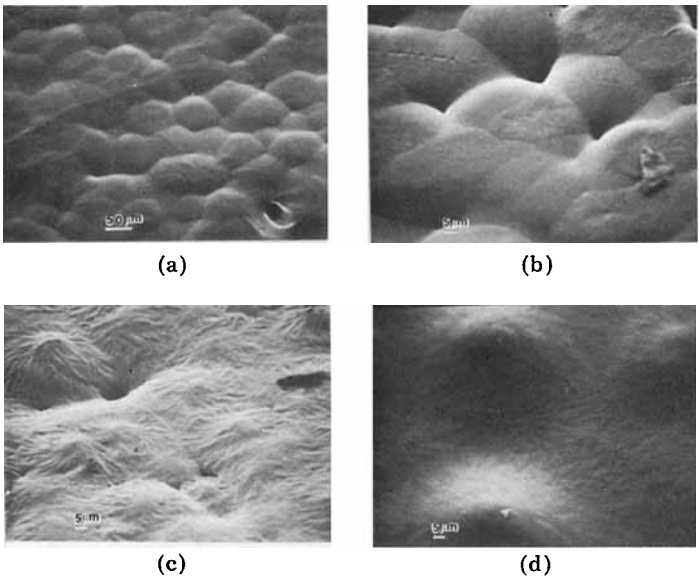

Fig. 14. Scanning electron micrographs of the (a) prepolymer, (b) 0.5-Mrad, (c) 10-Mrad, and (d) 16-Mrad materials.

information about the melt state. Even in the melt, the 0.5-Mrad sample shows a small amount of birefringence indicating that there is some order remaining in the system mainly due to crosslinking at the double bonds. However, the 4-Mrad and 12-Mrad samples show a relatively larger amount of local birefringence which can be attributed to freezing in order which is likely due to crosslinking along the crystalline main chain. Although melting of the crystals may occur at high irradiation doses (>8 Mrad), since the crosslinking process is quite in-

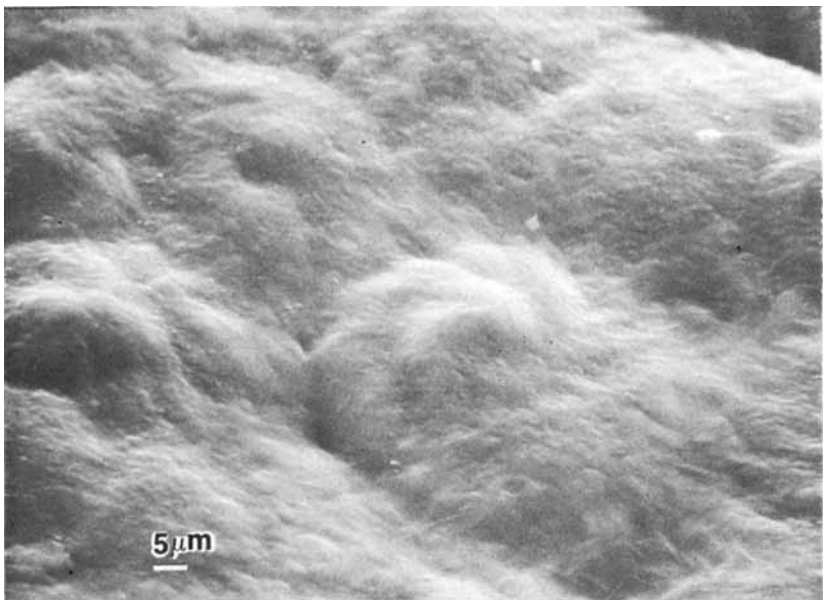

Fig. 15. Scanning electron micrograph of a melted and recrystallized 0.5-Mrad sample.

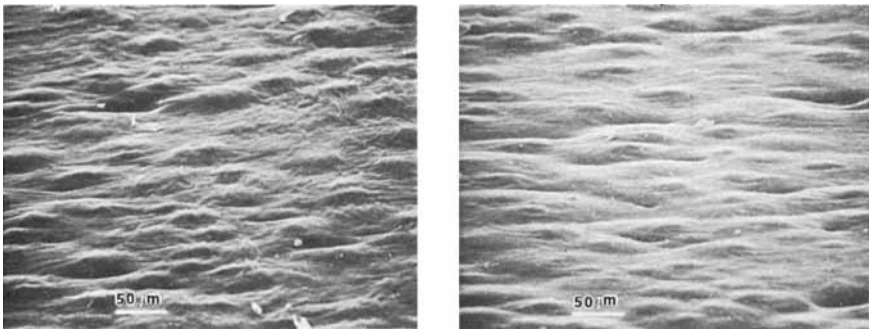

(a) (b)

Fig. 16. Scanning electron micrographs of (a) a 0.5-Mrad sample deformed at 270% elongation and (b) a 12-Mrad sample deformed at 200% elongation.

stantaneous, crosslinking of the melted but still aligned molecules takes place in the melt state thereby preserving order in the melt.

Isothermal Crystallization Kinetics

Isothermal crystallization studies were carried out using a polarizing microscope and a photodiode eyepiece to attempt to quantify the effect of crosslinking (radiation dose) on the fusion process. The materials were heated to 60°C, i.e., above the melting temperature for 5 min in a hot stage and cooled rapidly to a predetermined crystallization temperature. As crystallization occurs, depolarized light is transmitted through the analyzer and the photodiode monitors the changes in light intensity. From these data information regarding the induction time and rate of crystallization as a function of electron beam dose was easily obtained through the analysis procedures discussed via Avrami[11–13], Magill,[14,15] and Binsbergen.[16]

Data obtained from crystallization kinetics measurements at 25°C and 35°C are shown in Figures 17 and 18. The data were plotted using the general Avrami equation, and the straight lines obtained indicate that the data fit the equation quite well. For a given temperature, for example at 25°C, as electron beam dose increases, the rate of crystallization decreases. This is principally due to the increase in the number of crosslinks which are present in the crystallizable component and serve as restrictions to the crystallization process. Similar behavior is also seen at a higher crystallization temperature as expected. As shown in Figure 18, for a given irradiation dose, the induction time increases with crystallization temperature, as is also expected. This is due to a decrease in supercooling which reduces the driving force towards crystallization. It is also apparent that the increase in crystallization temperature has a more significant effect on the higher dosage samples. This, too, can be attributed to a further decrease in supercooling at higher irradiation doses due to a lower melting point. For example, for a 0.5-Mrad material T_m = 52°C while T_m = 48°C for a 12-Mrad material. Such a strong dependence on supercooling is not uncommon in many polymer systems. As expected, crystallization kinetics studies in the deformed state (50% and 100% elongations) showed that the induction time at each deformation ratio was lower than that for the undeformed case. This behavior can

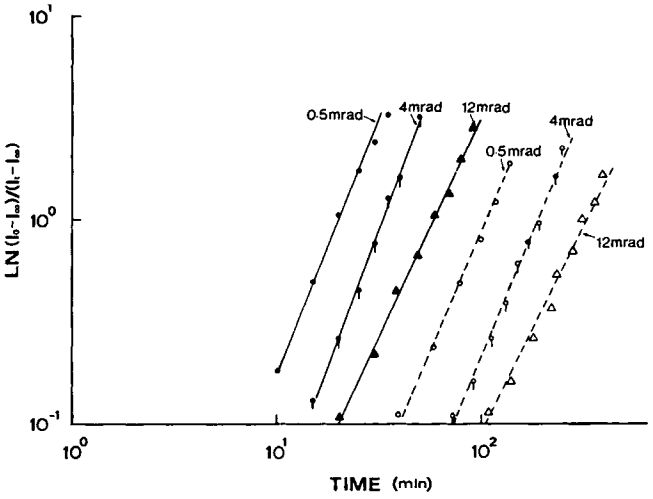

Fig. 17. Plot of ln $[(I_0 - I_\infty)/(I_0 - I_t)]$ vs. time for 0.5-Mrad, 4-Mrad, and 12-Mrad materials in isothermal crystallization experiments. (——) 25°C, (- - - -) 35°C. I_0, I_∞, and I_t represent the values of background, final, and time dependent depolarized light intensities, respectively.

be explained in terms of the relationship $T_m = \Delta H/\Delta S$, where ΔH is the heat of fusion and ΔS represents the entropy of fusion. When the sample is deformed, the molecules become aligned, and the entropy of the system is lowered. From the relationship mentioned above, it can be seen that this causes an increase in the melting temperature, which in turn corresponds to an increase in the degree of supercooling for a fixed crystallization temperature. Hence, the induction time decreases due to an increase in the driving force for crystallization. It should be mentioned, however, that a systematic relationship between extension ratio and induction time could not be obtained. That is, significant scatter existed; however, there was no doubt about the observation of the reduced induction time for deformed systems relative to undeformed cases, and this is in line with other workers who have studied strain induced crystallization in more detail.[17–19]

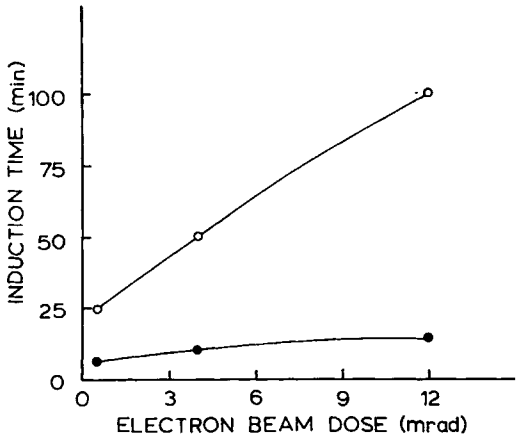

Fig. 18. Plot of induction time vs. electron beam dose in isothermal crystallization experiments (●) 25°C; (○) 35°C.

Properties of Prepolymer Crosslinked above the Melt

The results discussed so far have been concerned with network systems obtained by crosslinking the prepolymer at ambient conditions. Since it was strongly implied that melting occurred at high irradiation doses and caused changes in the properties and structure, it was of interest to study similar network systems that were crosslinked in the melt or liquid state. That is, the prepolymer was melted prior to crosslinking and then crosslinked in the melt state. Network systems were obtained by crosslinking the prepolymer with electron beam doses up to 4 Mrad and the final recrystallized and crosslinked films were analyzed in terms of their properties and superstructure.

Mechanical Studies above the Melt

The stress–strain plot of these systems measured above T_m are shown in Figure 19. The modulus increases from 4.8×10^5 Pa to 8.5×10^5 Pa as irradiation dose is raised up to 4 Mrad. This would directly be due to the increase in the degree of crosslinking as previously discussed. It is noted that the moduli values are of the same magnitude as those observed at similar temperatures but for prepolymer films crosslinked below T_m. Since these systems can also be classified as a network system, the stress–strain data were also plotted in the classical rubber elasticity equation, and the results are shown in Figure 20. The linear region indicates that up to an elongation of 125% classical theory is again followed while at higher elongations a deviation occurs, which is probably due to nongaussian behavior. Extension–retraction experiments in the region where

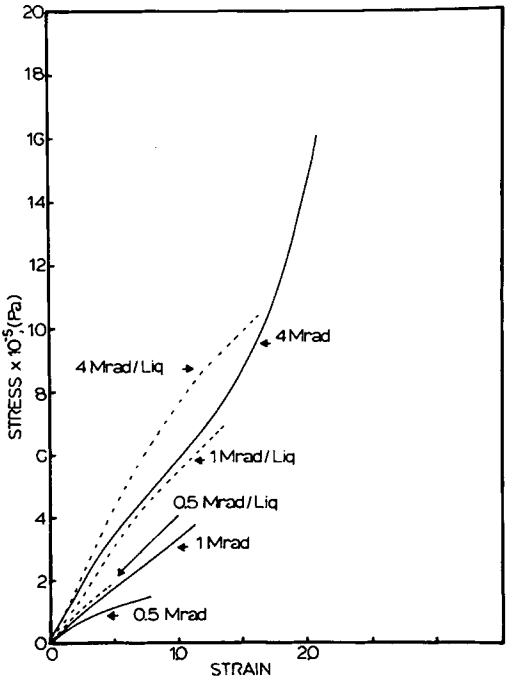

Fig. 19. Stress vs. strain curves above the melting temperature of the prepolymeer crosslinked in the melt state. These are shown by the the dashed lines (e.g., 4 Mrad/LIQ). Solid lines represent corresponding systems crosslinked below the melting temperature.

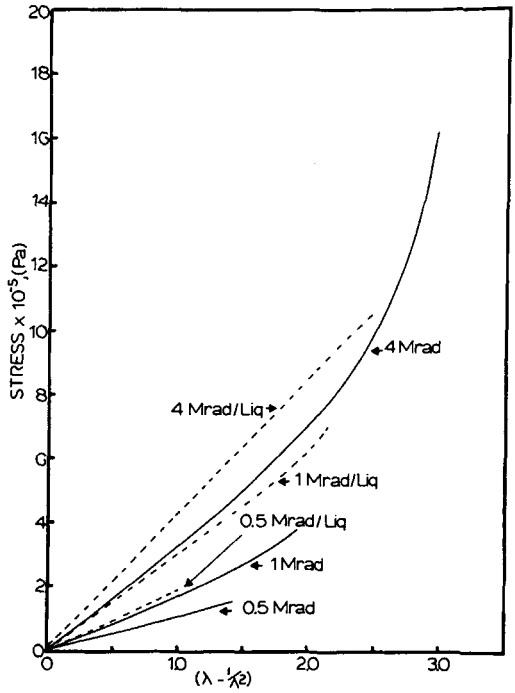

Fig. 20. Stress vs. $(\lambda - 1/\lambda^2)$ plot from stress–strain data obtained above the melting temperature of the prepolymer crosslinked in the melt state. Solid lines represent corresponding systems crosslinked below the melting temperature.

classical rubber-elasticity theory holds showed that these networks obtained by crosslinking the prepolymer above the melt had very low hysteresis as before.

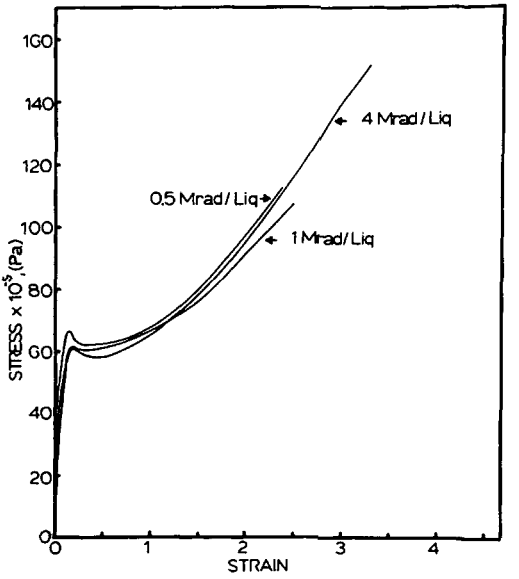

Fig. 21. Stress vs. strain curves at room temperature (i.e., below melting temperature) of the prepolymer crosslinked in the melt state. Modulus = 8×10^{-7}–10×10^{-7} Pa.

Mechanical Properties Determined below the Melt

Figure 21 shows the stress–strain plot obtained at room temperature of the prepolymer irradiated in the melt state for dosages ranging between 0.5 Mrad and 4 Mrad. It was found that the modulus and the yield stress have values that are *approximately half* of that found in the corresponding materials that were crosslinked below the melt. This is likely due to a lower amount of crystallinity present in the systems crosslinked above the melt. For example, the prepolymer crosslinked in the melt state with an irradiation dose of 0.5 Mrad has a 25% lower heat of fusion per gram than the prepolymer crosslinked at room temperature with the same irradiation dose. Certainly, the argument of differences in crosslinking would not account for this in view of the fact that the degree of crosslinking is reflected by the modulus in the melt state and this is the same order of magnitude for the materials crosslinked below T_m. A comparison of the mechanical properties of the systems crosslinked above and below the melt are shown in Table III.

Morphological Studies of Prepolymer Crosslinked above the Melt

Interestingly, the optical micrographs of the 0.5 Mrad/LIQ and 4 Mrad/LIQ between cross-polarizers show anisotropic spherulitic nature and when gradually heated, at a temperature of around 45°C, banded spherulites are more clearly observed. An example of this texture is shown in Figure 22. This behavior was also observed using SALS. The H_v small angle light scattering patterns of the 0.5 Mrad/LIQ and 4 Mrad/LIQ show four-leaf clover patterns which confirm the spherulitic superstructure. On gradually heating these systems, at 45°C, they show an H_v SALS pattern that has bands surrounding the four-leaf clover pattern. These bands are likely due to the periodic twisting of the lamella, which cause banded spherulites.

Figure 23 shows the scanning electron micrograph of the 4 Mrad/LIQ sample. As is noted clearly from these data and those above, crosslinking in the melt does not limit the later formation of a spherulitic superstructure. These spherulites were of a somewhat larger size than before, but to account for this would be unjustified in view of not truly knowing the nature of the cooling history following passage through the electron beam system.

Optical microscopy studies performed on the above materials at 60°C (i.e.,

TABLE III
Results of Mechanical Testing at Room Temperature

Material	Modulus (Pa)	Yield stress (Pa)
Prepolymer crosslinked at room temperature:		
(a) 0.5 Mrad	2.4×10^8	125×10^5
(b) 2 Mrad	2.4×10^8	140×10^5
(c) 4 Mrad	2.4×10^8	130×10^5
(d) 10 Mrad	2.26×10^8	75×10^5
Prepolymer crosslinked in the melt state:		
(e) 0.5 Mrad/LIQ	1×10^8	67×10^5
(f) 4 Mrad/LIQ	8×10^7	63×10^5

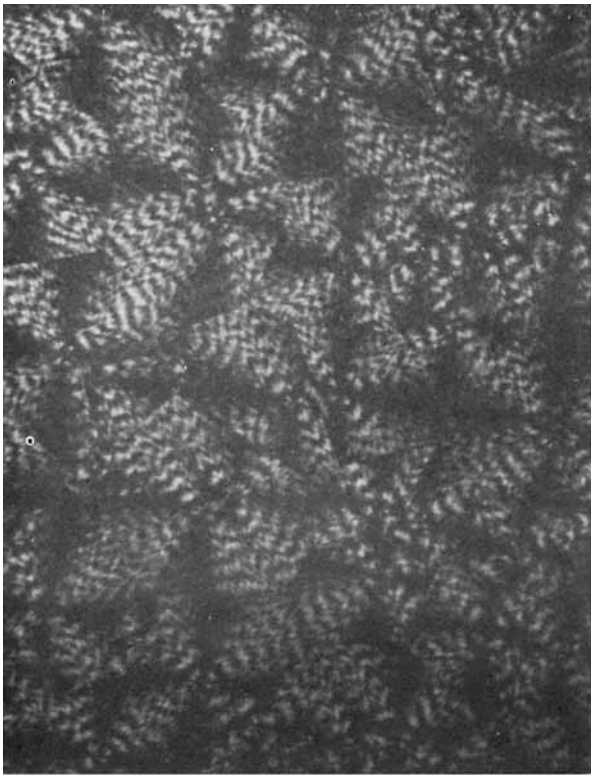

Fig. 22. Polarizing optical micrograph at 43°C (i.e., below T_m) of the prepolymer crosslinked in the melt state at 4 Mrad.

above the melt) showed that when both the 0.5-Mrad and 4-Mrad samples are observed between cross-polarizers at 60°C, no light is transmitted through indicating that there is *no order* in these systems *in the melt state.* This is in contrast to the 0.5-Mrad and 4-Mrad samples that were crosslinked at room temperature, which showed the presence of some order even in the melt state. The fact that no order exists in the systems crosslinked above the melt can be clearly explained as due to very little order being present in the system when the crosslinking is actually taking place.

Isothermal Crystallization Studies of Prepolymer Crosslinked above the Melt

Isothermal crystallization studies were carried on these network systems in order to again monitor the effect of crosslinking above and below the melting temperature. Using the depolarized light intensity technique, it was found that for a given crystallization temperature there is a slightly greater induction time for the prepolymer crosslinked below the melt. This result was rather surprising since it was initially expected that the prepolymer crosslinked above the melt would have a higher induction time due to the total random nature of the molecules at the time of crosslinking. At this time, we can offer no suitable explanation for this behavior.

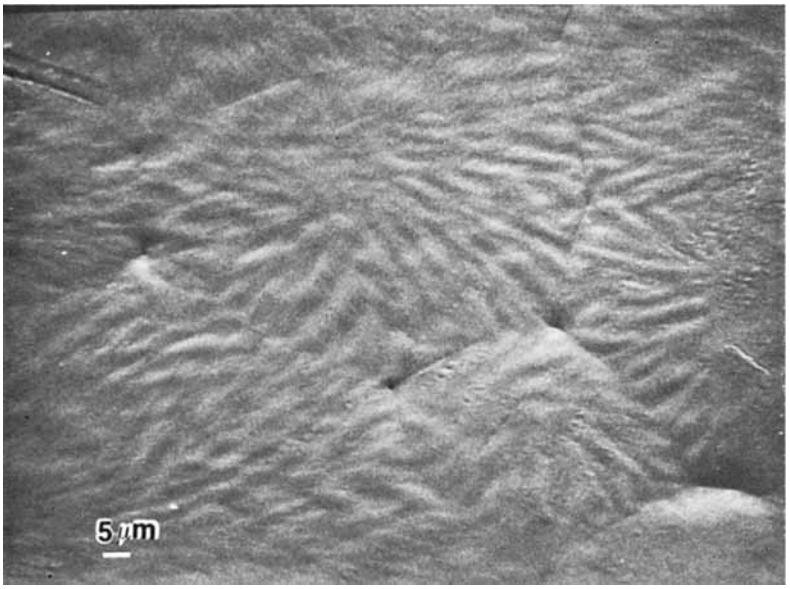

Fig. 23. Scanning electron micrograph of the prepolymer crosslinked in the melt state at 4 Mrad.

CONCLUSIONS

Prepolymer Crosslinked below the Melt

1. The superstructure of the network systems is clearly spherulitic in nature due to the initial spherulitic texture of the prepolymer. At irradiation doses lower than 8 Mrad, the surface texture is fairly smooth. As the irradiation dose is further increased, the surface texture becomes fibrous. This textural change at higher doses is believed to be due to the fact enough thermal energy is provided to melt the system, and on recrystallization the change in surface texture occurs.

2. Polarizing optical microscopy studies above the melting point clearly indicate that, at electron beam doses lower than 4 Mrad, crosslinking takes place mainly at the double bonds, which are outside the crystal lattice. However, at electron beam doses greater than 4 Mrad, crosslinking also occurs at locations along the main polymer chains which are inside the crystal lattice. This phenomena is also supported by gel fraction measurements.

3. On deformation, the higher dose materials show more recoverability due to the higher degree of crosslinking.

4. Above the crystalline melting point and up to an elongation of 125%, the networks follow classical rubber elasticity theory and classical photoelasticity theory. However, the addition of a tetrafunctional monomer creates a system that is non-gaussian in nature and rubber elasticity theory is not followed.

5. Below the melting point, there is a change in the mechanical properties as electron beam dose increases. These changes are attributed to the difference in crosslinking mechanisms; that is, crosslinking at the double bonds occurs outside the crystal while additional crosslinking along the main chain (at higher doses) promotes crosslinking within the crystallite and at other locations outside the crystal.

6. Isothermal crystallization kinetics studies clearly show that, as electron beam dose increases, (1) the induction time increases and (2) the rate of crystallization decreases. This is due to the additional amount of crosslinks which act as restrictions to the crystallization process.

Prepolymer Crosslinked above the Melt

1. The superstructure of these systems lead to banded spherulites. Also, the size of the spherulites seem to be somewhat larger than the spherulites of the corresponding system, which is crosslinked below the melt.

2. Polarizing optical microscopy above the melt shows that there is no order present in the melt state. This indicates that at the time when crosslinking occurs a totally random system exists. This is in contrast to the prepolymer crosslinked below the melt, which shows a measurable amount of order in the melt state.

3. Mechanical testing above the melting temperature shows that at elongations up to 125% classical rubber elasticity theory is followed implying that a gaussian network behavior is present.

4. Isothermal crystallization studies show that these systems have a lower induction time compared to the corresponding system crosslinked below the melt.

References

1. J. H. Saunders and K. C. Frisch, *Polyurethanes, Chemisty and Technology, Part II Technology*, Wiley, New York, 19xx.
2. W. K. Walsh and B. S. Gupta, *J. Coated Fabrics*, **7**, 253–262 (1978).
3. F. J. Gasparrini, *J. Coated Fabrics*, **9**, 6 (1979).
4. J. P. Guarino and E. P. Tripp, *Polym. Prepr., Am. Chem. Soc., Div. Organ. Coat. Plast., Chem.*, **39**, 9 (1978).
5. B. S. Gupta, W. S. McPeters, and W. M. Walsh, *J. Coated Fabrics*, **9**, 12–25 (1979).
6. K. Park and G. L. Wilkes, *Polym. Prepr., Am. Chem. Soc., Div. Organ. Coat. Plast., Chem.*, **41**, (1979).
7. O. W. Smith, J. E. Weigel, and D. J. Trecker, U.S. Patent 3,700,643 (to Union Carbide Corporation) (1972).
8. G. L. Wilkes, *J. Macromol. Sci. Rev., Macromol. Chem.*, **C10** (2), 213 (1974).
9. L. R. G. Treloar, *The Physics of Rubber Elasticity*, Oxford University Press, London, 1967.
10. R. S. Stein and M. B. Rhodes, *J. Appl. Phys.*, **31**, 873 (1960).
11. M. Avrami, *J. Chem. Phys.*, **7**, 1103 (1939).
12. M. Avrami, *J. Chem. Phys.*, **8**, 212 (1940).
13. M. Avrami, *J. Chem. Phys.*, **9**, 177 (1941).
14. J. H. Magill, *Polymer*, **2**, 221 (1961).
15. J. H. Magill, *Polymer*, **3**, 34, 43, 655 (1962).
16. F. L. Binsbergen, *J. Macromol. Sci. Phys.*, **B4**(4), 837 (1970).
17. G. S. Y. Yeh and K. Z. Hong, *Polym. Eng. Sci.*, **19**(6), 395 (1979).
18. W. Wu, *Polym. Eng. Sci.*, **19**(6), 391 (1979).
19. T. M. Remec and R. J. Gaylord, *Polym. Eng. Sci.*, **19**(6), 406 (1979).

Received March 10, 1981
Accepted April 27, 1981